Biosensors and Bioelectronics 25 (2010) 2447–2453

Contents lists available at ScienceDirect

Biosensors and Bioelectronics

journal homepage: www.elsevier.com/locate/bios

Morpholino-functionalized silicon nanowire biosensor for sequence-specific label-free detection of DNA

Guo-Jun Zhang*, Zhan Hong Henry Luo, Min Joon Huang, Guang Kai Ignatius Tay, Eu-Jin Andy Lim

*Institute of Microelectronics, A*STAR (Agency for Science, Technology and Research), 11 Science Park Road, Singapore 117685, Singapore*

ARTICLE INFO

Article history:
Received 26 January 2010
Received in revised form 1 April 2010
Accepted 2 April 2010
Available online 9 April 2010

Keywords:
Silicon nanowire
Biosensor
Surface functionalization
Hybridization detection
Morpholino
DNA

ABSTRACT

We investigated Morpholino-functionalized silicon nanowires (SiNWs) as a novel gene chip platform for the sequence-specific label-free detection of DNA. Morpholino attachment and subsequent Morpholino–DNA hybridization on silicon surface was characterized by X-ray photoelectron spectroscopy and fluorescence microscopy. The resultant Morpholino-modified surfaces showed high specificity of recognition for DNA. Subsequently, by using the same protocol, the surface of the SiNW biosensor was functionalized with Morpholino, and this was used for label-free Morpholino-DNA hybridization detection. Real-time measurements of the Morpholino-functionalized SiNW biosensor exhibited a decrease in a time-dependent conductance when complementary and mutant DNA samples were added. Furthermore, identification of fully complementary versus mismatched DNA samples was carried out by the Morpholino-functionalized SiNW biosensor. We demonstrated that DNA detection using the Morpholino-functionalized SiNW biosensor could be carried out to the hundreds of femtomolar range. The Morpholino-functionalized SiNWs show a novel biosensor for label-free and direct detection of DNA with good selectivity, and a promising application in gene expression.

1. Introduction

Gene sensors are devices used in the fields of molecular biology and medicine for basic research, disease diagnostics and drug discovery (Graber et al., 1998; Lipshutz et al., 1999; Wang, 2000; Lockhart and Winzeler, 2000; Boon et al., 2000; Hirschhorn et al., 2000; Wang et al., 2001; Kelly et al., 1999). In gene sensors, surface hybridization between nucleic acid probes, immobilized on a substrate, and complementary nucleic acid targets, occurs at a solid–liquid interface. Although the specificity of the hybridization is affected by many factors like buffer ionic strength, temperature and incubation time, it is, on the other hand, highly dependent on the level of complementary bases between the probes and target nucleic acids. Detection of a specific target nucleic acid requires the immobilization of the specific probe, which is optimal for the capture of the target nucleic acids. Thus to ensure optimal hybridization, hybridization conditions need to be tailored to individual sets of probes.

With the development of microelectronic technology, microelectronic devices on small scale have been developed as gene sensors, like DNA field effect transistor (FET) (Fritz et al., 2002; Uslu et al., 2004; Poghossian et al., 2005; Song et al., 2006; Sakata and Miyahara, 2007). Over the past several years, SiNW biosensors have been developed as sensitive and label-free analytical assays (Patolsky et al., 2006) in detecting metal ions (Cui et al., 2001; Zhang et al., 2007), nucleic acids (Hahm and Lieber, 2004; Li et al., 2004, 2005; Bunimovich et al., 2006; Gao et al., 2007; Zhang et al., 2008a,b, 2009), proteins (Cui et al., 2001; Zheng et al., 2005; Stern et al., 2007; Chua et al., 2009) and viruses (Patolsky et al., 2004). Silicon nanowire (SiNW) biosensors are one of FET-based devices capable of label-free detection of nucleic acids. Compared to the conventional FET devices, SiNW gene sensors have much higher sensitivity due to very small dimension of nanowires constrained to tens of nanometers or less, and thus resulting in large surface-to-volume ratio.

Realization of DNA sensors requires the immobilization of nucleic acid probes to silicon surface of a FET. Hybridization of target nucleic acids with nucleic acid probes elicits a change in resistance, and in turn the current flowing through the FET. DNA, as a common probe, has been attached to silicon surface using different functionalization strategies. However, the negatively charged DNA molecule is not suitable as a sensing element for highly sensitive measurement in SiNW biosensor because the biosensors are electronic devices that operate as FET, which in principle, depend on charge variation induced by binding of target nucleic acids. Electrostatic hindrance between DNA duplex, which does not benefit hybridization, is another drawback. Moreover, high salt conditions required for DNA–DNA hybridization are not applicable for

* Corresponding author. Tel.: +65 6770 5390; fax: +65 6774 5754.
E-mail address: zhanggj@ime.a-star.edu.sg (G.-J. Zhang).

0956-5663/$ – see front matter © 2010 Elsevier B.V. All rights reserved.
doi:10.1016/j.bios.2010.04.001

Table 1
Morpholino and DNA sequences used in this work.

Morpholino	5′-H_2N-AACCACACAACCTACTACCTCA-3′
Complementary DNA	5′-TGAGGTAGTAGGTTGTGTGGTT-3′
One-base mismatched DNA	5′-TGAGGTAGTAGGATGTGTGGTT-3′
Non-complementary DNA	5′-ATGCATGCATGCATGCATGCAA-3′
Cy 3-labeled complementary DNA	5′-Cy 3-TGAGGTAGTAGGTTGTGTGGTT-3′
Cy 3-labeled non-complementary DNA	5′-Cy 3-ATGCATGCATGCATGCATGCAA-3′

real-time monitoring using surface electric field-based FET sensors. As an alternative, peptide nucleic acid (PNA), which is neutral, was employed for detection of DNA in SiNW biosensors (Hahm and Lieber, 2004; Li et al., 2004, 2005; Bunimovich et al., 2006; Gao et al., 2007; Zhang et al., 2008a,b). The PNA-functionalized SiNW biosensors were reported to have an obvious sensitivity compared to the DNA-modified ones (Zhang et al., 2009). Nevertheless, PNA is expensive in synthesis, and more severely, the length of the nucleobases to be synthesized is restricted, which is unsuitable for application such as gene expression that requires a longer probe length. Morpholino oligos, unique gene knockdown reagents, were discovered in 1985 by Summerton (Summerton, 1989; Summerton and Weller, 1997). Morpholino subunit comprises of a nucleic acid base, a morpholine ring and a non-ionic phosphorodiamidate intersubunit linkage. Different from PNA, Morpholino has a flexibility in length synthesis and is thus more advantageous. Furthermore, Morpholino excels in the properties of stability, nuclease-resistance, efficacy, long-term activity, water-solubility, low toxicity and exquisite specificity as compared to DNA and PNA. Very recently, Tercero et al. (2009) have reported formation of Morpholino monolayers on gold surface and surface hybridization between Morpholino and DNA. This illustrates that Morpholino is becoming an interesting probe molecule for biosensor development.

In this paper, we demonstrate Morpholino attachment onto silicon substrate grown with a native oxide by covalent binding, subsequent Morpholino-DNA hybridization on the same surface, and finally label-free detection of DNA in real-time by means of the Morpholino-functionalized SiNW biosensor. We investigate the Morpholino layer on the silicon surface using X-ray photoelectron spectroscopy (XPS), the hybridization of DNA with the Morpholino-modified surface, and the stability of the Morpholino-modified surface. We show that the SiNW sensors functionalized with Morpholino are able to distinguish a single base mismatched sequence. In general, the Morpholino-functionalized SiNW biosensor, which is capable of DNA sequence variations detection, could show potential as a novel gene sensor in gene expression and disease diagnostics.

2. Experimental

2.1. Materials

3-Aminopropyltriethoxysilane (99%) and glutaraldehyde solution (50 wt.% in H_2O) were obtained from Sigma–Aldrich (St. Louis, MO). Morpholino oilgomers, purified by precipitation, were purchased from Gene Tools LLC (Philomath, OR). The DNAs were purchased from 1st BASE Oligos (Singapore). The Morpholino used for immobilization was amine-terminated at its 5′ end. Each of Morpholino and DNAs was 22-mer in length.

All the sequences employed in the study are shown in Table 1. Morpholino is immobilized on the SiNW surface as a capture probe molecule, whereas complementary DNA, one-base mismatched DNA and non-complementary DNA are three targets used for real-time measurements. Cy 3-labeled complementary DNA and Cy 3-labeled non-complementary DNA are another two targets used for fluorescence illustration.

2.2. SiNW device fabrication

The silicon nanowire devices were fabricated using a n-doped silicon-on-insulator (SOI) substrate as previously reported (Chua et al., 2009). 8-in. SOI wafers with 700 Å silicon and 1450 Å buried oxide layers were used for silicon nanowire fabrication. Silicon fins of ~100 nm widths were patterned using deep ultra-violet lithography and reactive-ion etching. An oxidation at 900 °C was further employed to scale down the nanowire widths to ~70 nm. Next, a phosphorus implantation was done at 30 keV for a dose of 5×10^{13} cm^{-2}, and activated at 1000 °C for 30 s in N_2. 4000 Å of high-density plasma oxide was used for nanowire passivation, and contact holes were opened at both ends of the nanowires. A high dose (5×10^{15} cm^{-2}) phosphorus implantation and activation was conducted to obtain n+ regions. Ohmic contacts were realized after TaN/AlSiCu metallization and annealing at 420 °C for 30 min. Finally, nitride/oxide/nitride passivation layers were deposited to protect the metal lines, leaving the metal pads and active nanowire sensor areas exposed. The nanowires were released by dry etching of the Si_3N_4/SiO_2 passivation layers followed by wet etching of the remaining SiO_2. The devices were stored in a dessicator cabinet for 5 days, which allowed native oxide growth on the nanowire surface.

2.3. Morpholino attachment onto SiNW surface

The SiNW chip was immersed into 2% 3-aminopropyltriethoxysilane (APTES) in a mixture of ethanol/water (95%/5%, v/v) for 2 h. The chip was washed with absolute ethanol for three times and blow-dried. The chip was then treated with 2.5% glutaraldehyde solution in water for 1 h, and thoroughly washed with water. 10 μM Morpholino in 1 × SSC was incubated with the chip in a humid atmosphere at room temperature overnight. Unreacted Morpholino probes were removed by washing the substrate with 1 × SSC for three times.

2.4. Electrical real-time detection of DNA using Morpholino-functionalized SiNW sensor

Electrical measurements of SiNW conductances were performed by a HP parameter analyzer (HP-4155A) via an Alessi REL-6100 probe station (Cascade Microtech, Beaverton, OR). A short pulse voltage of 0.1 V was applied to the SiNW device and the current through the SiNW was measured. One data point was taken every 1 s in order to reduce possible heating effects due to power dissipation through the SiNW device.

To be able to detect DNA using the Morpholino-functionalized SiNW sensor, an acrylic reservoir was mountained on the chip to allow for fluid exchange for detection. Fluid supply and return were carried out by Syringe pump through Tygon tubes. Such a macro-scale solution chamber allows for sufficient solution for real-time detection. The nanowire conductance was recorded as a function of time while the chip was exposed to target DNA.

To allow sufficiently long Debye length, 0.01 × SSC buffer solution was used in the experiment, as described previously (Zhang et al., 2008a,b, 2009).

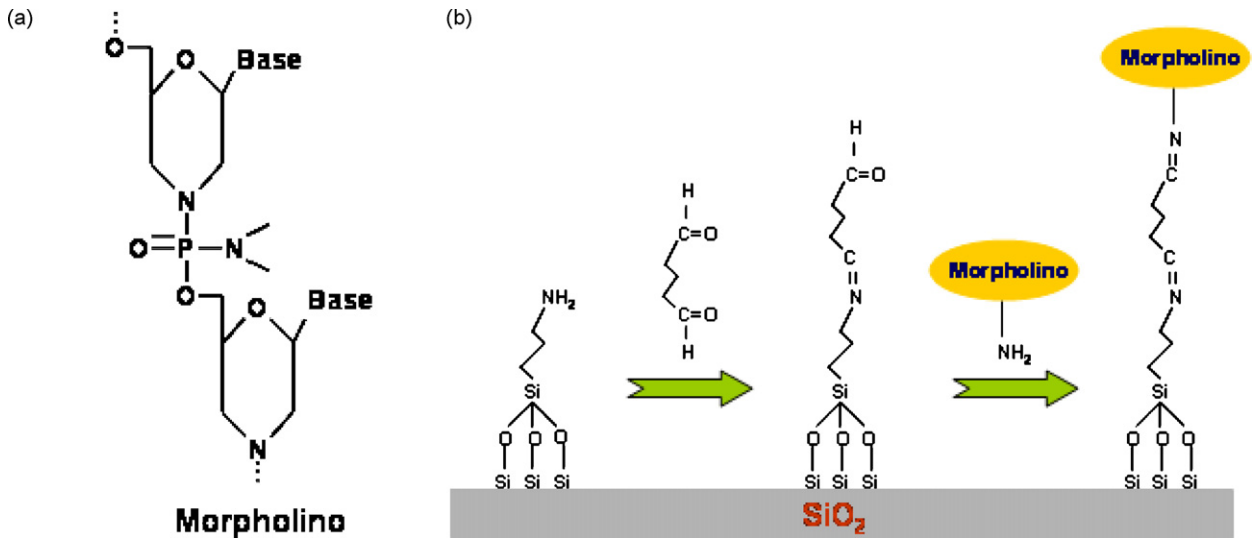

Fig. 1. Structure of Morpholino oligomers and covalent attachment of Morpholino on silicon surface. (a) Uncharged Morpholino oligo structure. (b) Schematic diagram of the stepwise functionalization of Morpholino on the SiO_2-terminated silicon surface.

2.5. X-ray photoelectron spectroscopy

X-ray photoelectron spectra were obtained on a PHI Quantera SXM Scanning X-ray Microprobe (ULVAC-PHI, Inc., Japan) using monochromatic Al Ka X-rays (1486.6 eV). Pass energy of 224 eV and 55 eV were used for survey scan and high resolution (narrow) scan, respectively. The spot size was 200 μm. The sample surface was tilted at 45° with respect to the analyzer detector.

2.6. Fluorescence microscopy

The fluorescence microscopy was performed using an Olympus BX61 epi-fluorescence microscope equipped with a color cooled CCD camera SPOT-RT Slider (Diagnostic Instruments, USA), a 100 W HBO bulb, and Olympus fluorescence filter sets (U-MWU2, U-MWB2, U-MF2).

3. Results and discussion

3.1. Surface characterization of Morpholino layer on silicon substrate

DNA attachment on the common (0 0 1) and (1 1 1) surfaces of silicon has been studied by using a long-chain alkene terminated with a reactive groups (Strother et al., 2000a,b; Böcking et al., 2006; Voicu et al., 2004; Pike et al., 2002). Likewise, PNA attachment to the silicon surface has also been achieved with the similar strategy (Zhang et al., 2008a,b). On the other hand, direct functionalization of silicon substrate with an oxide layer is a common way of realizing DNA and PNA attachment by the silane chemistry (Li et al., 2004, 2005; Gao et al., 2007; Zhang et al., 2004, 2009). However, to date, little is known on Morpholino attachment on silicon substrates. To explore Morpholino-based biosensors, Morpholino immobilization on silicon substrates is particularly attractive. Thanks to the fact that silicon naturally oxidizes in air to generate a native oxide, an oxide-based surface functionalization is adopted in this work. A Morpholino subunit structure is shown in Fig. 1a. Each subunit is comprised of a nucleic acid base, a morpholine ring and a non-ionic phosphorodiamidate intersubunit linkage. The chemistry employed for Morpholino attachment onto silicon surface is illustrated in Fig. 1b. The silicon surface covered with oxide is reacted with APTES, yielding an amine-modified surface. The Morpholino-modified with amine groups at its 5′ end is covalently immobilized on the silicon surface through a bi-functional glutaraldehyde. The Morpholino-modified surface is therefore produced for the subsequent hybridization with DNA.

XPS was used to characterize the resulting Morpholino layer on the silicon surface. Different from DNA whose backbone is phosphate, Morpholino's backbone is phosphorodiamidate. The silicon surface coated with Morpholino was expected to be modified with carbon, oxygen, nitrogen, and phosphorus species, of which nitrogen and phosphorus can be indicative of Morpholino because environmental carbon or oxygen may be introduced to the surface due to contamination. To immobilize Morpholino on the silicon surface for XPS analysis, Si(1 0 0) bulk wafer was cut into 1 cm × 1 cm pieces. The silicon substrate was ultrasonically cleaned in acetone and ethanol for 5 min each, followed by oxidation in a solution prepared by mixing hydrogen peroxide, ammonium hydroxide and water in a 1:1:4 volumetric ratio. After soaking for 5 min, the substrate was rinsed with water and blow-dried. The substrate was immersed into 2% APTES in a mixture of ethanol/water (95%/5%, v/v) for 2 h. The substrate was washed with absolute ethanol for three times and blow-dried. The chip was then treated with 2.5% glutaraldehyde solution in water for 1 h, and thoroughly washed with water. 10 μM amine-modified Morpholino in 1 × SSC was incubated with the substrate in a humid atmosphere for 12 h. Fig. 2 shows the wide energy XPS spectra after each modification including the bare silicon substrate (1), the APTES-modified silicon surface (2), the glutaraldehyde-modified silicon surface (3), and the Morpholino-modified silicon surface (4). Bulk silicon surface gave rise to Si 2p, O 1s and C 1s peaks. After the silicon substrate was modified with APTES, the amine groups were terminated on the surface and an obvious peak (N 1s) was obtained. Further introduction of aldehyde groups increased ratio of carbon and subsequently decreased ratio of nitrogen, but still the N 1s peak was clearly obvious. After immobilization of Morpholino, the silicon, carbon, nitrogen, oxygen and phosphrous peaks were present on the Morpholino-modified surface. However, the phosphrous peak was slightly weak due to contrast to the remarkable Si 2p peak. Importantly, the phosphrous peak was not observed from the other three surfaces. The comparison of XPS characterization on the different surfaces indicates that the surface functionalization is realized as anticipated.

XPS spectra of Si 2p, C 1s, O 1s, N 1s and P 2p regions of the morpholino-functionalized surface are illustrated in Fig. S1. The C 1s spectrum in Fig. S1a shows two peaks at 284.3 eV and at 284.5 eV,

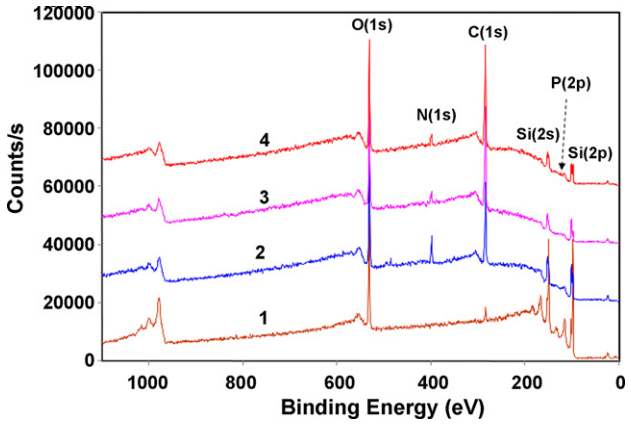

Fig. 2. XPS spectra (survey scan) of the different functionalized silicon surfaces. (1) Bare silicon surface. (2) APTES-modified surface. (3) Aldehyde-modified surface. (4) Morpholino-modified surface.

contributed by bulk C–C group and C–O group, respectively. A bulk Si 2p peak at 101.8 eV in Fig. S1b indicates that there is a significant oxidation on the silicon surface (Si–O bond). In addition, another bulk Si 2p peak at 101.5 eV and 98.3 eV corresponding to Si–C and Si–Si bonds, respectively, were obtained. Likewise, a very large O 1s peak at 531.4 eV in Fig. S1c was observed, which depicts clear evidence of the presence of the native oxide on the silicon surface. The P 2p and N 1s peaks in Fig. S1d and e are indicative of Morpholino molecules. The P 2p peak at 133.9 eV was obtained, which corresponds to the binding energy of P in backbone of Morpholino. In the N 1s region, we observed three peaks at 398.6, 398.9, and 401.3 eV that are assigned to P–N, C–N and C=N bonds, respectively. The peak of P 2p is smaller than that of N 1s, which is expected from the relative content of N and P in Morpholino structure shown in Fig. 1a. Moreover, the N 1s is also attributed to C=N group in the link molecules.

To further verify the stepwise immobilization of Morpholino on the silicon surface, the thickness of APTES- and morpholino-modified surfaces was measured by Ellipsometer. Since the refractive index varies depending on the density and the molecular orientation, it is difficult to measure the thickness of a layer, where the refractive index is unknown. In the work, we assume that the layer formed on the surface after each step is a single layer and refractive index of silicon dioxide is used for measurement on these two different surfaces. The results show that the APTES layer gave rise to ~22 Å in thickness, and the Morpholino layer further resulted in ~66 Å in thickness. The APTES layer measured using Ellipsometer is slightly thicker than that (14.96 Å) obtained using vacuum ultra-violet spectroscopic Ellipsometer (Goyal et al., 2008). The Morpholino used in the study is 22-bp long, corresponding to approximately 70 Å in length. The thickness of the Morpholino layer immobilized on the silicon surface almost matches the intrinsic length of the Morpholino, further indicating that the morpholino has been attached onto the silicon surface.

3.2. Hybridization of DNA to the Morpholino-modified silicon surface

Fluorescence micrographs were taken to illustrate hybridization of the immobilized Morpholino with DNA on silicon surface. The silicon substrate was treated with APTES and glutaraldehyde as mentioned above. 10 μM Morpholino in 1 × SSC buffer was spotted manually on the aldehyde-modified Si surface. 1% bovine serum albumin (BSA) in phosphate-buffered saline (PBS) was used to block the unreacted aldehyde groups on the surface after the Morpholino-spotted substrate was incubated in a humid atmosphere for 12 h.

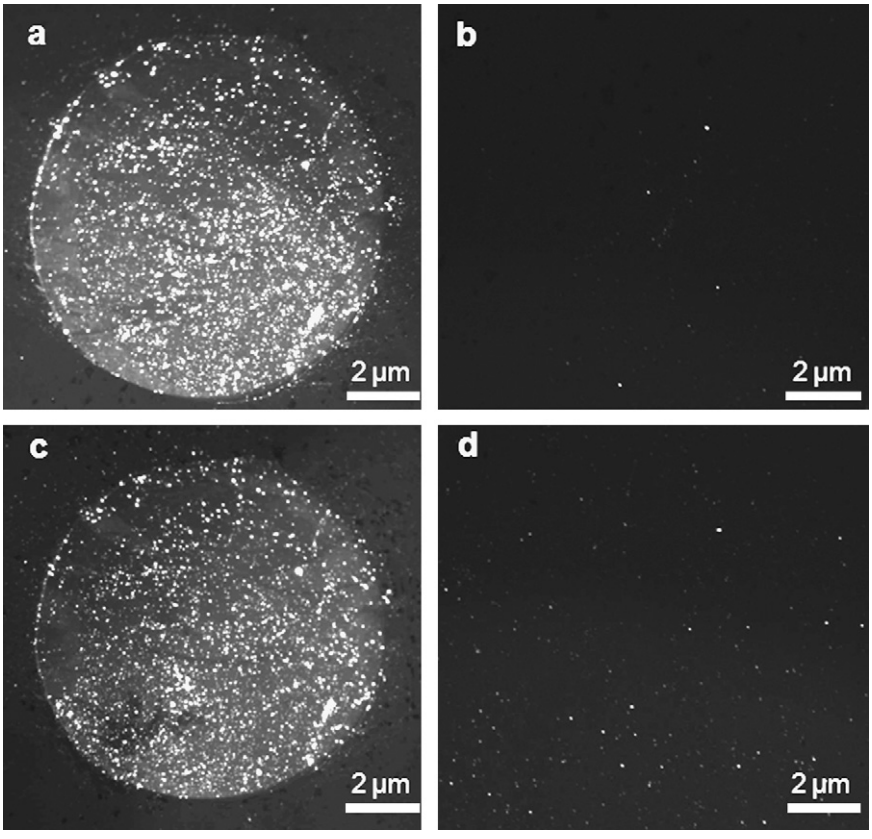

Fig. 3. (a) Fluorescence image of a complementary Cy 3-labeled DNA hybridized to the Morpholino immobilized on silicon surface. (b) Denaturation. (c) Fluorescence image of the same Cy 3-labeled DNA re-hybridized to the Morpholino. (d) Denaturation and hybridization with a non-complementary Cy 3-labeled DNA.

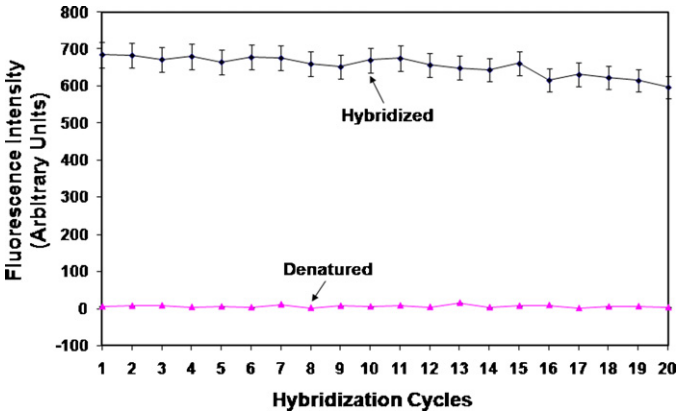

Fig. 4. Stability of the Morpholino-functionalized silicon surface during 20 cycles of hybridization and denaturation.

1 μM the fully complementary DNA labeled with Cy 3 in 1 × SSC was incubated with the substrate to allow hybridization with the spotted Morpholino for 1 h, and after washing the hybridization event was finally imaged by fluorescence microscope. A spot was clearly observed, indicating that DNA was exclusively bound to the spotted Morpholino area. The potential regeneration of the Morpholino-modified surface was investigated by denaturing Morpholino-fully complementary DNA duplex, subsequently re-hybridizing the same fluorescently labeled complementary DNA to the Morpholino-spotted surface. Denaturation was conducted by placing the substrate in an 8.3 M urea solution at room temperature for 5 min followed by a rinse with water. As confirmed again by fluorescence microscope, no spot was visible in Fig. 3b, exhibiting that the labeled oligonucleotides were removed. As could be seen from Fig. 3c, further hybridization with the same labeled oligonucleotides resulted in the fluorescence spot detectable with almost no change in intensity compared to that for the first hybridization when the Morpholino-modified substrate was used for another set of hybridization experiment under the same condition. To evaluate the sequence specificity, denaturation and re-hybridization with a Cy 3-labeled non-complementary DNA followed by imaging did not show the fluorescent spot on the surface (Fig. 3d). For the fluorescence measurements, the silicon covered with its native oxide is not well-adapted because of its high refractive index. This explains the very low intensity of the fluorescence and the inhomogeneity of the two spots in Fig. 3a and c (Bras et al., 2004). These results demonstrate that Morpholino attachment on the silicon surface is successful, and Morpholino and DNA hybridization occurs subsequently.

3.3. Stability of Morpholino-modified silicon surface

To investigate stability of Morpholino-modified silicon surface, the identical spot was utilized for further hybridization by denaturing Morpholino-fully complementary DNA duplex and re-hybridizing the same Cy 3-labeled DNA to the Morpholino-modified surface. A series of 20 successive cycles were conducted in order to capture the fluorescence intensity of the same spot after hybridization in each cycle, as reported previously (Zhang et al., 2006). Fig. 4 shows stability of the Morpholino-modified silicon surface during 20 hybridization and denaturation cycles. The fluorescence intensity after 20 cycles is ~87% of the initial value, corresponding to a loss of 0.6% per cycle. These findings are in good agreement with those obtained on DNA-modified silicon surface (Strother et al., 2000a,b). As described earlier, the fluorescence intensity was also measured after denaturation of each of the 20 cycles. It was found that the intensity was negligible compared to background. A coefficient of variation of 5% was obtained for 20 cycles of hybridization and denaturation.

3.4. Real-time detection of DNA using Morpholino-functionalized SiNW

Having established the surface chemistry for Morpholino immobilization on the silicon substrate, a SiNW sensor functionalized with the same Morpholino sequence was exposed to a buffer solution (0.01 × SSC) containing 1 nM of various DNAs, and its conductance was recorded as function of time. The n-typed SiNW used in the work was fabricated by self-limiting oxidation process of silicon beams patterned using conventional deep UV photolithography. The SiNW array chip consists of 36 clusters of electrically addressable and well-ordered SiNWs separated by a 200 μm spacing; each cluster is composed of five individually addressable nanowires and each nanowire has its own contact pads. The width of each SiNW is appropriately 50–60 nm. As illustrated in Fig. 5a, five well-aligned nanowires are formed in one cluster with the corresponding electrical contacts. A fluidic reservoir was adhered to the SiNW chip for solution exchange using the double-side tape which was sticked to the bottom of the reservoir. Unlike fluidic microchannel, the reservoir is able to hold sufficient liquids inside and improve the solution exchange rate as desired. A single device was employed for biosensing in the experiments. Fig. 5b is a schematic showing the Morpholino-funtionalized SiNW sensor for detection of DNA. Addition of negatively charged DNA to the sensor surface due to Morpholino–DNA hybridization, leads to an accumulation of charges on the surface, thereby lowering the conductance of SiNW. Similar to PNA, Morpholino has a high affinity for DNA because it is neutral and able to eliminate electrostatic repulsion between Morpholino–DNA duplex. The use of Morpholino as capture probes can produce ultralow background electric charges. In the meantime, the neutral character of Morpholino backbone allows hybridization to take place at low ionic strength, minimizes the build-up of a strong electrical field at the SiNW surface, and thereby reduces the background, producing a high signal/noise ratio.

Conductance versus time data recorded with a Morpholino-functionalized SiNW sensor indicate a remarkable decrease in conductance after addition of 1 nM fully complementary DNA in 0.01 × SSC buffer solution (Fig. 5c), as expected for a typical n-type device. The decrease in conductance is consistent with an increase in negative surface charge because of binding of negatively charged oligonucleotides to the surface. Negligible conductance change was observed when the same concentration of non-complementary DNA solution was introduced to the Morpholino-functionalized SiNW surface. This implies that the sequence specificity of Morpholino–DNA duplex using the label-free electrical measurement is confirmed and non-specific adsorption on the sensor surface can be neglected. PNA has a high affinity for DNA and show maximum promises for discriminating between single base differences. To investigate whether Morpholino has the same capabilities, the Morpholino-functionalized SiNW sensor was exposed to 1 nM one-base mismatched target DNA in 0.01 × SSC buffer solution. Addition of the single base mutant resulted in a small but detectable response in conductance. These results demonstrate that the conductance decrease is attributed to formation of Morpholino–DNA duplex on the SiNW surface, and in addition, the Morpholino-functionalized SiNW sensor shows high-affinity applications in SNPs (single nucleotide polymorphisms).

To further demonstrate the sensitivity of the Morpholino-functionalized SiNW biosensor, concentration-dependent data using various complementary DNA in 0.01 × SSC buffer solution were recorded. Fig. 5d shows conductance response versus time for

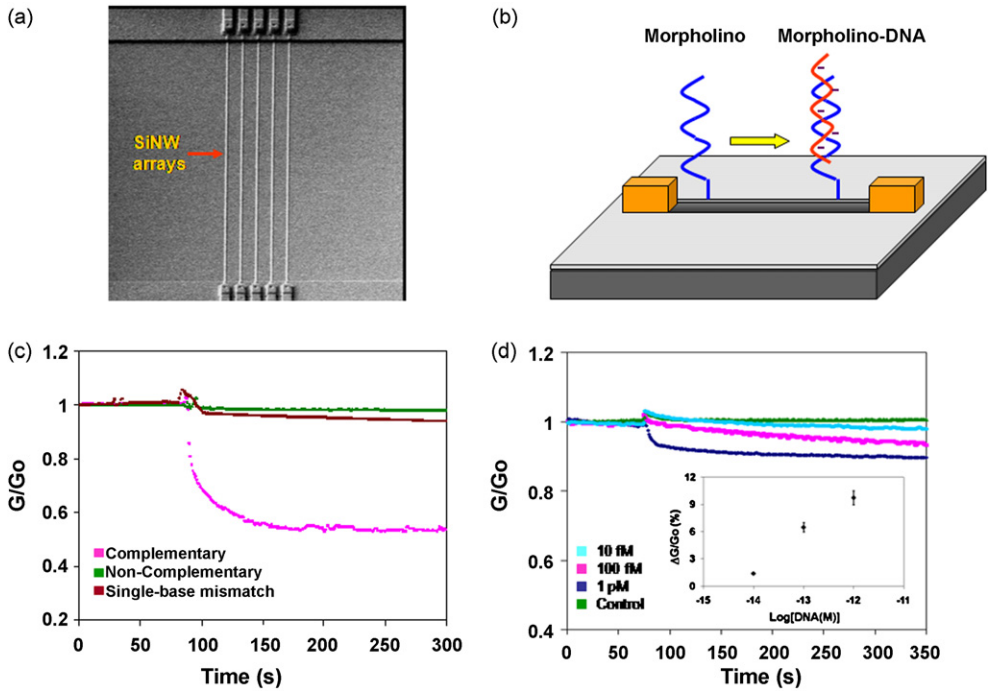

Fig. 5. (a) SEM micrograph of one cluster of five 90 μm long, ~50–60 nm wide, parallel SiNW arrays with 2 μm spacing inbetween. (b) A schematic illustration of a single SiNW sensing device. Morpholino is covalently immobilized on the SiNW surface. Hybridization of Morpholino–DNA leads to accumulation of negative charges on the surface, thereby inducing conductance decrease in n-type SiNW. (c) Real-time conductance response for a Morpholino-functionalized SiNW sensor during injection of 1 nM complementary, non-complementary and one-base mismatched DNAs. (d) Conductance versus time for a Morpholino-functionalized SiNW sensor during injection of various concentrations of complementary DNA solution and DNA-free buffer solution. Inset shows sensitivity versus logarithm of DNA concentration.

various complementary DNA in 0.01 × SSC buffer solution. A control was carried out, in which addition of the same buffer solution without DNA to a Morpholino-functionalized SiNW sensor after the baseline was stabilized in 0.01 × SSC exhibited negligible change in conductance. Known DNA concentrations ranging from 1 pM to 10 fM were injected and the corresponding conductance changes were observed as a function of time. Sensitivity was determined by running a series of experiments with a signal-to-noise ratio of 3. The inset shows sensitivity versus logarithm of DNA concentration. The results reveal that DNA concentrations as low as 100 fM can be detected with the Morpholino-functionalized SiNW biosensor in real-time. The calculated relative standard deviation (RSD) from the data is 8.4%, which shows a satisfactory reproducibility for label-free and real-time detection of DNA using the Morpholino-functionalized SiNW biosensor.

To compare sensing performance using Morpholino or DNA as the probe, real-time detection of DNA using DNA-functionalized SiNW sensor was carried out. In this experiment, a DNA probe molecule whose sequence is same as Morpholino's was immobilized on the SiNW surface replacing the Morpholino, the specific conductance changes were recorded as a function of time due to DNA–DNA hybridization after addition of DNA to the DNA-functionalized SiNW surface. As shown in Fig. S2, the DNA-functionalized SiNW sensor gave rise to an obvious drop in conductance when 1 nM DNA was added. Addition of 100 pM still resulted in a detectable signal, whereas addition of 10 pM induced a negligible conductance change. The results show that 100 pM can be effectively detected by the DNA-functionalized SiNW surface, which is three orders of magnitude lower than that obtained by the Morpholino-functionalized SiNW sensor.

4. Conclusions

In summary, we have demonstrated that the Morpholino-functionalized SiNW function as a novel, selective and label-free DNA biosensor at concentrations down to hundreds of femtomolar range. We have described the method for covalently coupling Morpholino to silicon surface and hybridizing complementary DNA with the immobilized Morpholino. The yielded Morpholino silicon surface is selective and stable towards the denaturation and re-hybridization circle. We have shown that the Morpholino-functionalized SiNW biosensor could distinguish the complementary versus mismatched DNA sequences. Moreover, it should be possible to use longer Morpholino as probe molecules and extend this approach to the detection of longer target sequences, which is applicable in determining the expression profiles of many genes at the same time. We believe that an integrated SiNW biosensor based on functionalization of Morpholino on the SiNW surface that could enable high-throughput DNA detection will be developed for applications in the fields of gene expression.

Acknowledgments

The authors would like to thank Dr. Takashi Tanii in the Faculty of Science and Engineering, Waseda University for discussion on thickness measurement using Ellipsometer, Mr. Jay Huiyi Chua and Ms. Ru-Ern Chee for their assistance with real-time measurements. We also acknowledge Ms. Dao Thuy Khanh Linh Kathy at Data Storage Institute in Singapore for her assistance with XPS spectra.

Appendix A. Supplementary data

Supplementary data associated with this article can be found, in the online version, at doi:10.1016/j.bios.2010.04.001.

References

Böcking, T., Kilian, K.A., Gaus, K., Gooding, J.J., 2006. Langmuir 22, 3494–3496.

Boon, E.M., Ceres, D.M., Drummond, T.G., Hill, M.G., Barton, J.K., 2000. Nat. Biotechnol. 18, 1096–1100.
Bras, M., Dugas, V., Bessueille, F., Cloarec, J.P., Martin, J.R., Cabrera, M., Chauvet, J.P., Souteyrand, E., Garrigues, M., 2004. Biosens. Bioelectron. 20, 797–806.
Bunimovich, Y.L., Shin, Y.S., Yeo, W.-S., Amori, M., Kwong, G., Heath, J.R., 2006. J. Am. Chem. Soc. 128, 16323–16331.
Chua, J., Chee, R.E., Agarwal, A., Wong, S.M., Zhang, G.-J., 2009. Anal. Chem. 81, 6266–6271.
Cui, Y., Wei, Q.Q., Park, H.K., Lieber, C.M., 2001. Science 293, 1289–1292.
Fritz, J., Cooper, E.B., Gaudet, S., Sorger, P.K., Manalis, S.R., 2002. Proc. Natl. Acad. Sci. U.S.A. 99, 14142–14146.
Gao, Z.-Q., Agarwal, A., Trigg, A.D., Singh, N., Fang, C., Tung, C.-H., Fan, Y., Buddharaju, K.D., Kong, J.-M., 2007. Anal. Chem. 79, 3291–3297.
Goyal, D.K., Pribil, G.K., Woollam, J.A., Subramanian, A., 2008. Mater. Sci. Eng. B 149, 26–33.
Graber, J.H., OïDonnel, M.J., Smith, C.L., Cantor, C.R., 1998. Curr. Opin. Biotechnol. 9, 14–18.
Hahm, J.-I., Lieber, C.M., 2004. Nano Lett. 4, 51–54.
Hirschhorn, J.N., Sklar, P., Lindblad-Toh, K., Lim, Y., Ruiz-Gutierrez, M., Bolk, S., Langhorst, B., Schaffner, S., Winchester, E., Lander, E.S., 2000. Proc. Natl. Acad. Sci. U.S.A. 97, 12164–12169.
Kelly, S.O., Boon, E.M., Barton, J.K., Jackson, N.M., Hill, M.G., 1999. Nucleic Acids Res. 27, 4830–4837.
Li, Z., Chen, Y., Li, X., Kamins, T.I., Nauka, K., Williams, R.S., 2004. Nano Lett. 4, 245–247.
Li, Z., Rajendran, B., Kamins, T.I., Li, X., Chen, Y., Williams, R.S., 2005. Appl. Phys. A 80, 1257–1263.
Lipshutz, R.J., Fodor, S.P.A., Gingeras, T.R., Lockhart, D.J., 1999. Nat. Genet. 21, 20–24.
Lockhart, D.J., Winzeler, E.A., 2000. Nature 405, 827–836.
Patolsky, F., Zheng, G., Hayden, O., Lakadamyali, M., Zhuang, X., Lieber, C.M., 2004. Proc. Natl. Acad. Sci. U.S.A. 101, 14017–14022.
Patolsky, F., Zheng, G., Lieber, C.M., 2006. Nat. Protoc. 1, 1711–1724.
Pike, A.R., Lie, L.H., Eagling, R.A., Ryder, L.C., Patole, S.N., Connolly, B.A., Horrocks, B.R., Houlton, A., 2002. Angew. Chem. Int. Ed. 41, 615–617.
Poghossian, A., Cherstvy, A., Ingebrandt, S., Offenhäusser, A., Schöning, M.J., 2005. Sens. Actuators B 111–112, 470–480.
Sakata, T., Miyahara, Y., 2007. Biosens. Bioelectron. 22, 1311–1316.
Song, K.-S., Zhang, G.-J., Nakamura, Y., Furukawa, K., Hiraki, T., Yang, J.-H., Funatsu, T., Ohdomari, I., Kawarada, H., 2006. Phys. Rev. E 74, 041919.
Stern, E., Klemic, J.F., Routenberg, D.A., Wyremebak, P.N., Turner-Evans, D.B., Hamilton, A.D., LaVan, D.A., Fahmy, T.M., Reed, M.A., 2007. Nature 445, 519–522.
Strother, T., Hamers, R.J., Smith, L.M., 2000a. Nucleic Acids Res. 28, 3535–3541.
Strother, T., Cai, W., Zhao, X.S., Hamers, R.J., Smith, L.M., 2000b. J. Am. Chem. Soc. 122, 1205–1209.
Summerton, J., 1989. In: Brakel, C. (Ed.), Discoveries in Antisense Nucleic Acids. Portfolio Publishing Co., The Woodlands, TX.
Summerton, J., Weller, D., 1997. Antisense Nucleic Acid Drug Dev. 7, 187–195.
Tercero, N., Wang, K., Gong, P., Levicky, R., 2009. J. Am. Chem. Soc. 131, 4953–4961.
Uslu, F., Ingebrandt, S., Mayer, D., Böcker-Meffert, S., Odenthal, M., Offenhäusser, A., 2004. Biosens. Bioelectron. 19, 1723–1731.
Voicu, R., Boukherroub, R., Bartzoka, V., Ward, T., Wojtyk, J.T.C., Wayner, D.D.M., 2004. Langmuir 20, 11713–11720.
Wang, J., 2000. Nucleic Acids Res. 28, 3011–3016.
Wang, J., Polsky, R., Xu, D., 2001. Langmuir 17, 5739–5741.
Zhang, G.-J., Agarwal, A., Buddharaju, K.D., Singh, N., Gao, Z.-Q., 2007. Appl. Phys. Lett. 90, 233903.
Zhang, G.-J., Chua, J., Chee, R.E., Agarwal, A., Wong, S.M., 2009. Biosens. Bioelectron. 24, 2504–2508.
Zhang, G.-J., Chua, J., Chee, R.E., Agarwal, A., Wong, S.M., Buddharaju, K.D., Balasubramanian, N., 2008a. Biosens. Bioelectron. 23, 1701–1707.
Zhang, G.-J., Song, K.-S., Nakamura, Y., Ueno, Funatsu, T., Ohdomari, I., Kawarada, H., 2006. Langmuir 22, 3728–3734.
Zhang, G.-J., Tanii, T., Funatsu, T., Ohdomari, I., 2004. Chem. Commun. 7, 786–787.
Zhang, G.-J., Zhang, G., Chua, J., Chee, R.E., Wong, E.H., Agarwal, A., Buddharaju, K.D., Singh, N., Gao, Z.Q., Balasubramanian, N., 2008b. Nano Lett. 8, 1066–1070.
Zheng, G., Patolsky, F., Cui, Y., Wang, W.U., Lieber, C.M., 2005. Nat. Biotechnol. 23, 1294–1301.